Desalination and Water Treatment
www.deswater.com

doi: 10.5004/dwt.2017.20245

65 (2017) 304–312
February

Adsorption of red nylosane solution on natural materials

Aoumria Ouldmoumna[a,b,*], Nouredine Benderdouche[b], Laurence Reinert[c], Benaouda Bestani[b], Laurent Duclaux[c]

[a]*LMAE, Faculté des Sciences et de la Technologie, université de Mascara B.P. 763, Route Mamounia, Mascara 29000, Algeria, email: aouldmoumna@yahoo.fr*
[b]*LSEA2M, Faculté des Sciences et de la Technologie, Université Abdelhamid Ibn Badis de Mostaganem (UMAB), B.P. 188, Mostaganem 27000, Algeria*
[c]*LCME, Polytech Annecy-Chambéry, Université de Savoie, 73376 Le Bourget du Lac Cedex, France*

Received 29 June 2016; Accepted 3 October 2016

ABSTRACT

This study attempts to identify the characteristics of obtained biosorbents to assess their suitability for water treatment. The adsorption tests were conducted in a continuous mode. The prepared biosorbent exhibits excellent adsorption capacities in the liquid phase vis-à-vis red nylosane. Indeed, the ultimate capacities of adsorption (q_e) were calculated using the Langmuir linearization, which is 83.33 mg g^{-1} for the two biosorbents, *Cynara cardunculus* (CARD) and *Eucalyptus globulus* (EUCA), and 76.92 mg g^{-1} for *Prunus cerasifera* (PRUN). The adsorption equilibrium constants, 0.008 for CARD, 0.0058 for EUCA and 0.0052 for PRUN, present a strong affinity of these biosorbents for red nylosane, which has an acidic pH. A characterization of materials by determining accessible surface to methylene blue, the microporosity by the iodine and surface area by Brunauer–Emmett–Teller method. The determination of acid and base chemical functions that are present in the three biosorbents is by FTIR analysis and pH_{PZC}. The spontaneous and endothermic process with all materials is used. The results prove that the three biosorbents studied are very useful in the treatment of contaminated water with micropollutants such as red nylosane dye.

Keywords: Biosorbents; Ultimate capacity; Kinetics; Red nylosane; Isothermal

1. Introduction

Effluents of textile industries are part of wastewater. These releases are organic chemicals such as hydrocarbons, aromatics, and colorants in fact; they are considered as hazardous micropollutants, since they are less remarkable. The health of living organisms is deteriorating slowly; their lives are shortened; their offspring may eventually develop malformed; and their probability of being is affected by "cancer" rate increases.

The science and technology is one of the improving processes of pollution that is why many researchers have investigated the use of plants to extract heavy metals from water and soil [1]. Some plant species have shown a lucid resistance of some metals such as copper, zinc, and lead [2]. Several studies are performed to manufacture the adsorbents from vegetable wastes that aim to protect the environment as well as present good results vis-à-vis the fixation of some pollutants [3–7]. Recently, a number of studies have been performed for the adsorption of some dyes (acid and base metal complex reagents), sawdust, and other biosorbents: Hêtre [8,9], rubber wood [10], the core of cherry, pine [9,11], cedar [12], a mixture of sawdust and clay [13], Indian rosewood [14], sawdust spruce magnetically modified [15,16], oak [17], *Pycnoporus sanguineus* [18], eco-friendly biosorbent [19]; Mediterranean green alga *Enteromorpha* spp. [20], Mansonia wood sawdust [21] and pineapple leaf powder[22]. In our study, we have chosen to work with the state gross waste of three plants that are *Cynara*

* Corresponding author.

cardunculus (Cardoon; CARD), *Prunus cerasifera* (Prunier; PRUN) and *Eucalyptus globulus* (Eucalyptus; EUCA) in relation to their availability in our area. The pollutant is chosen to eliminate the synthetic dye red nylosane (RN) because synthetic dyes currently represent a relatively large group of chemical compounds found practically in all spheres of our daily life [23]. The world production of dyes is estimated at 700,000 tons/year, in which 140,000 are released in effluents during different steps of implementation and making [23]; these releases, especially dyes, are toxic to most living organisms.

The main purpose of this study is the preparation and characterization of biosorbents. Adsorbents tested the power and compare the performance in adsorption capacity between the three biosorbents. We have characterized and compared the performance of adsorption using UV-Vis spectrometry.

2. Materials and methods

2.1. Preparation of biosorbents

This current work focuses on determining the characteristics of obtained biosorbents with CARD, EUCA, and PRUN. Biomaterials adsorption of RN have been prepared and studied to set first their adsorption and physical parameters, and second their abilities of treating the polluted water. The biosorbent used in this study were prepared according to the experimental protocol decree by our laboratory [6]. First, the leaves of CARD, EUCA, and PRUN were thoroughly washed with laboratory-produced distilled water (5 μS/cm) and, then, dried in an oven at 60°C for 24 h. Finally, they were placed in the mill type (ball mill type: Croschop Viersen at 90 revolutions per minute). The porosity of biosorbents was sifted by sieves (212 mesh). After the recovery of the powders, they were directly used in our tests.

2.2. Adsorbate

The RN falls into the category of azo acid dyes, which is supplied by the Merck Company (Darmstadt, Germany); it is an acid dye; it tends to bind preferentially to the basic structures. The adsorbate used has a molecular weight of 587.97 g mol^{-1} and a dye content 35%–40%. The chemical structure of dye is depicted in Fig. 1.

2.3. Adsorption parameters

The adsorption of the biosorbents parameters has been determined by studying the adsorption of RN on these biosorbents as a function of time with a solution of initial concentration (100 mg L^{-1}). The adsorption of RN on biosorbents function of time determines the contact time adsorbent–adsorbate required to establish an adsorption equilibrium (pseudo-fast adsorption equilibrium). Biosorbent doses used for this were 2 to 20 g L^{-1}. The adsorption tests were performed under static conditions in a reactor in batch mode from 50 to 1000 mg L^{-1} with 25 ml of an aqueous solution of RN. The resulting suspension was stirred for 5–180 min. Centrifugation for the separation of the adsorbate and biosorbant was performed at 3,500 rpm for 15 min in a centrifuge (Hettich D-78532 Tuttlingen centrifuges, 6,000 U/min). The pH was studied in a range of 2–12. The residual concentrations of centrifuges are resolved using a spectrophotometer Jenway UV–visible spectrophotometer Model 6400 at 500 nm.

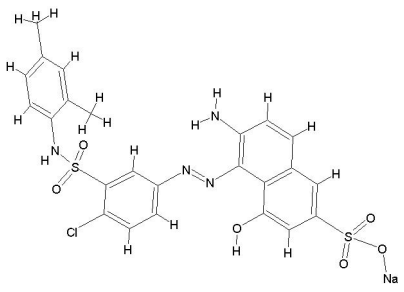

Fig. 1. Molecular structure of red nylosane (RN).

To identify the maximum adsorption capacity based on the initial concentration, an optimal dose of material is added to 25 mL of the solution. After stirring and centrifuging the solutions, they have been analyzed to determine the residual concentrations of RN. This mass was chosen for biosorbents because lying on the field of balance for the concentration range studied in this work. The adsorption capacity of biosorbent is calculated using Eq. (1):

$$q_e = \frac{(Co - Ce)\cdot V}{m} \quad (1)$$

where m is the mass of biosorbent used (g); V is the volume of the solution (mL); q_e is the apparent ability of adsorption (mg/g) of the material vis-à-vis the adsorbate; C_0 is the initial concentration of solution of RN (mg/l); and C_e is the residual concentration (mg/l) of the solution of RN.

2.4. Methods used for the characterization

2.4.1. Chemical functions of the surface using infrared spectroscopy

Mid-infrared transmittance measurements of the adsorbents (dye) studied were carried out on a NICOLET 380 FTIR spectrometer at room temperature in the 400–4000 cm^{-1} wave number range, with 2 cm^{-1} resolution. Pellets made of a mixture of 0.6 mg of biosorbent and 200 mg of KBr were pressed at 350 MPa, and oven-dried for 48 h at 110°C before the analysis.

2.4.2. Thermogravimetric analysis

Changes in the mass of biosorbents during decomposition and loss of volatile material that occurred upon heating were followed by thermogravimetry. Thermogravimetric analyses were performed in a Pyrox furnace coupled to a Mettler balance. Analyses were performed under air, from room temperature to 1,000°C with a heating rate of 4°C min^{-1}. Temperature and mass data were collected and processed by a computer devoted to the system.

2.4.3. Physical and chemical parameters

The values of iodine number, surface accessible to methylene blue, pH_{PZC} for the three biosorbents are made by the procedure described in our laboratory [3–6].

2.4.3.1. Iodine test

Iodine number is a widely used parameter for activated carbon testing for its simplicity and a rapid assessment of adsorbent quality. It gives an estimate of its surface area and porosity. Iodine concentration was determined volumetrically using 0.05 mol L^{-1} sodium thiosulfate with thyodene as an indicator at a residual iodine concentration of 0.01 mol L^{-1} according to ASTM D64 (1999) standard [24].

2.4.3.2. pH of zero point charge (pH_{PZC})

The pH_{PZC} is defined as the pH for which there is neutral charge on the surface of the adsorbent. A volume of sodium chloride solution (0.01 mol L^{-1}) was placed in capped bottles; the pH was adjusted from 2 to 12 by adding concentrated sodium hydroxide or hydrochloric acid. 0.15 g of biosorbent was then added to the NaCl solutions. After stirring magnetically for 48 h, the final pH was measured and plotted against the initial pH. The pH corresponding to the point of intersection with the pH (final) = pH (initial) was taken as the pH_{PZC} of the material.

2.4.3.3. Determination of the surface area accessible to methylene blue

Methylene blue is a typical dye applied to calculate the accessible surface of sorbents to large molecules. The available surface with methylene blue is calculated by the following equation:

$$S_{MB} = \frac{b.N.S}{M} \quad (2)$$

with S_{MB} is the surface area (m^2 g^{-1}), and b is maximum adsorption capacity (mg g^{-1}) based on a monolayer coverage. It can be determined from Langmuir model; N is Avogadro's number (6.023×10^{23} mol^{-1}); S is the surface occupied by a molecule of methylene blue (taken as 119 $Å^2$); and M is the molecular weight of methylene blue (319.86 g mol^{-1})

2.4.3.4. N_2 adsorption–desorption at 77 K

The N_2 adsorption–desorption isotherms of the activated carbons were measured using an automatic adsorption instrument (ASAP 2000, Micromeritics) at liquid nitrogen temperature (77 K). Prior to measurements, biosorbent samples were degassed at 80°C for 12 h under vacuum. The specific surface areas (S_{BET}) of the biosorbents were calculated using the Brunauer–Emmett–Teller (BET) equation by assuming the area of the nitrogen molecule to be 16.2 $Å^2$. The total pore volumes were estimated as the liquid volume of adsorbate adsorbed (N_2) at a relative pressure of 0.99 [25].

3. Results and discussion

3.1. Characterization of biosorbents and the dye used

Fig. 2 [6] shows the Fourier transform infrared (FTIR) spectra of the three biosorbents. The broad absorption band at 3,300–3,600 cm^{-1} with a maximum at about 3,400 cm^{-1} is characterized by the stretching vibration of hydrogen-bonded hydroxyl groups (from water).

The FTIR spectrum of the biosorbent shows bands at 2,935 cm^{-1} and 2,800 cm^{-1} arising from aliphatic C–H stretching (in an aromatic methoxyl group, in methyl and methylene groups of side chains) and from aromatic C–H stretching, respectively. The broad band observed in all spectra at ~1,044.2 cm^{-1} (Fig. 1) can be assigned to C–O stretching in acids, alcohols, phenols, ethers and/or esters groups [26]. The dominant peaks observed at 512 and 659 cm^{-1} suggest the presence of C–H rocking vibrations of cellulose. In the region 1,300–1,400 cm^{-1}, several absorption bands corresponding to stretching vibrations of C–N bonds are observed. A peak observed at 1,626 cm^{-1} corresponds to bending vibrations in the plane of H bonds. The band located at 1,830 cm^{-1} indicates the presence of C=O.

Identification of various functional groups present in the dye "Red Nylosane" is needed to understand the adsorption mechanism. FTIR spectrum (Fig. 3) dye shows the distinct picks at 3,500, 3,100, 1,620, 1,300–1,500, and 800–1,200 cm^{-1}. The broad and strong band ranging from 3,100 to 3,600 cm^{-1} due to overlapping of –OH and –NH stretching. Some picks observed at 1,620, 1,500, 1,400 and 1,300 cm^{-1} are attributed to C–H stretching and –NH bending. In the region 800–1,200 cm^{-1} confirm the presence of the halogen (Cl^-) and allongement Cetonic flexion.

The thermograms of the three materials (Fig. 4) [6] presents a first weight loss at low temperature (T < 100°C) attributed to the elimination of adsorbed water. It corresponds to about 10% for CARD and to about 5% for the

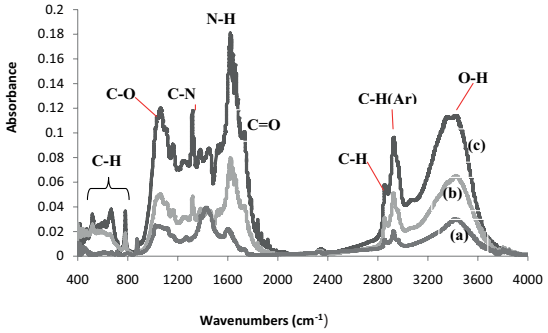

Fig. 2. FTIR spectra of the three biosorbents: (a) *Eucalyptus globulus*, (b) *Cynara cardunculus* and (c) *Prunus cerasifera*.

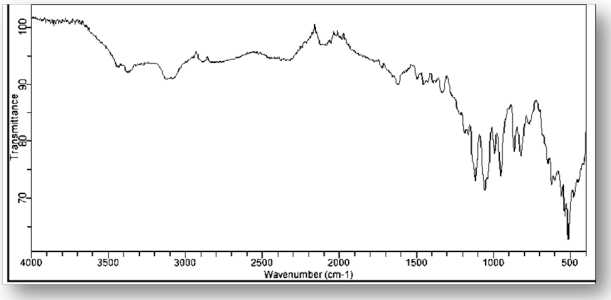

Fig. 3. FTIR spectra of the RN dye.

two other biosorbents. The first mass loss was attributed to the departure of physisorbed water and the second loss at ~100°C (100°C < T < 150°C) to the emission of chemisorbed water. The first stage of carbonization occurs in the temperature range of 200°C–500°C (70% loss) due to the eradication of volatile material rich in functional groups (lignin, hemicellulose and cellulose).

Table 1 [6] shows that the iodine number values were highest for CARD (535 mg g^{-1}) followed by EUCA (446 mg g^{-1}) and by PRUN (370 mg g^{-1}).

Surface accessible to methylene blue values were highest for CARD (746 m^2 g^{-1}) followed by EUCA (560 m^2 g^{-1}) and by PRUN (320 m^2 g^{-1}).

The pH_{PZC} values are very similar for all the biosorbents and closed to 6.5, indicating that these natural materials can be considered as close to neutral adsorbents. The BET surface area is highest for CARD in accordance with the iodine number values while those for the other two biosorbents are close.

3.2. Adsorption parameters

3.2.1. Effect of dose of adsorbent

Fig. 5 shows that high adsorption rates were obtained at a minimum dose of 8 g L^{-1} for EUCA, CARD and PRUN.

The percentage of removed RN increases initially very rapidly with the increase of adsorbent content (Fig. 5). As the adsorbent dose increases, the number of adsorbent particles increases; thus, more RN is attached to their surfaces. Beyond an adsorbent content of 8 g L^{-1}, the percentage of RN removed reached a constant value. A slight increase in uptake was observed when the dose was increased from 4 to 8 g L^{-1}. Any further addition of the adsorbent beyond this value did not cause any significant change in the adsorption.

3.3. Effect of pH on the adsorption of RN

Preliminary studies have shown that the adsorption capacity increases as the pH decreases. Therefore, this parameter must be an important variable that affects the adsorption process. In a series of beakers, we introduced 25 mL of known RN are introduced; the pH range was chosen to examine the evolution of the adsorption of this pollutant; the pH is adjusted if necessary with sodium hydroxide and concentrated hydrochloric acid to which was added a gross weight of the powder. The mixture was stirred for a specified period, then filtered and analyzed by spectrophotometer. The results of the variation in the rate of adsorption of RN function of pH are plotted in Fig. 6.

The best highest percentages of the RN eliminations are obtained at acidic pH values for all biosorbents. This can be explained on the basis of point of zero charge for the adsorbents studied. The pH_{PZC} is 6.50. At a pH less than this point, the load on the surface of biosorbent is positive, causing a greater electrostatic attraction of anions dye, leading to a higher adsorption for the RN. At a pH greater than pH_{PZC}, the surface of the material becomes negative, so there is a repulsion between the OH-ions in the solution and the negative charge of biosorbents thereby decreasing the adsorption. The increase in dye adsorption depends on the properties of the adsorbent surface and structure of the dye [27,28]. In our case study, this behavior clearly indicates that the RN

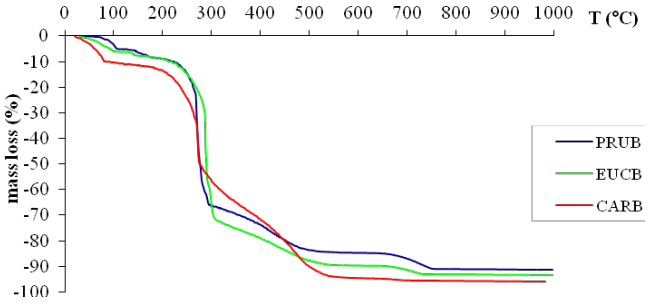

Fig. 4. Thermogravimetric curves of the three biosorbents.

Table 1
Characterization of the studied biosorbents

	Eucalyptus globulus	*Prunus cerasifera*	*Cynara cardunculus*
Iodine number (mg g^{-1})	446	370	535
Accessible surface methylene blue (m^2 g^{-1})	560	320	746
pH_{PZC}	6.37	6.80	6.25
S_{BET} (m^2 g^{-1})	14.0	13.8	22.0

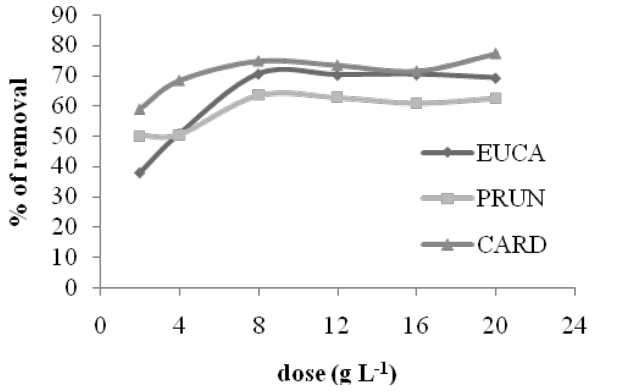

Fig. 5. Effect of biosorbent dose on the removal rate of RN (C_0 = 100 mg L^{-1}).

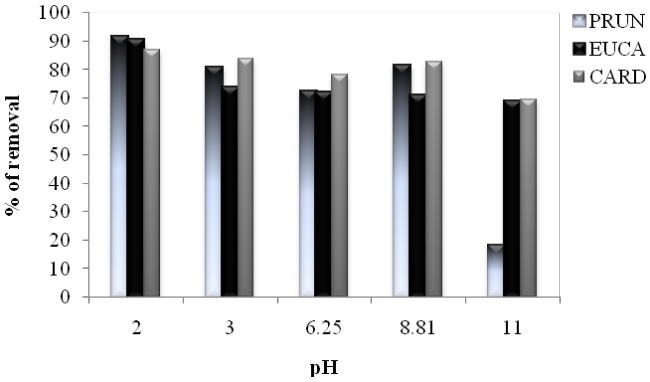

Fig. 6. Effect of pH on biosorption with C_0 = 100 mg L^{-1}.

is protonated in acidic medium, and by raising the pH of the dye removal is becoming weaker. Researchers have shown the possibility of development of the positive charge on the surface of biosorbent, which causes an inhibition of dye binding [29]. A decrease in the elimination of the dye is observed beyond basic pH and can be due to electrostatic repulsion. Similar behavior has been reported by other studies [29,30].

3.4. Adsorption kinetics

The study of biosorption of a compound in a biosorbent allows us to examine the influence of contact time on retention. This study was conducted to determine the target quantity of RN since from their initial contact until 180 min of agitation.

Fig. 7 shows that equilibrium is rapidly and totally accomplished of the RN with the biosorbent based on three materials (EUCA, PRUN and CARD). One can see that equilibrium was reached after a contact time of 120 min. It is assumed that sufficient time is allowed to reach equilibrium for all manipulations.

To investigate the controlling mechanism and the reaction order of the adsorption of RN onto the three materials prepared, the Lagergren pseudo-first-order and pseudo-second-order equations, and the intraparticle diffusion model were applied. The pseudo-first-order rate equation is given as:

$$\log(q_e - q_t) = \log q_e - (k_1/2.303)t \quad (3)$$

where q_t and q_e are the adsorption capacities at time t and at equilibrium (mg g^{-1}), respectively, and k_1 (min^{-1}) is the rate constant of the pseudo-first-order adsorption. Linear plots of $\log(q_e - q_t)$ against t give access to the rate constants k_1. The pseudo-second-order equation can be expressed as:

$$\frac{t}{q_t} = \frac{1}{k_2 q_e^2} + \frac{1}{q_e}t \quad (4)$$

where k_2 is the pseudo-second-order rate constant (mg g^{-1} min^{-1}). $k_2 q_e^2$ can be assumed as the initial adsorption rate as t goes to zero. The plot of t/q_t vs. t gives a straight line if second-order kinetics describes the biosorption process (Fig. 8).

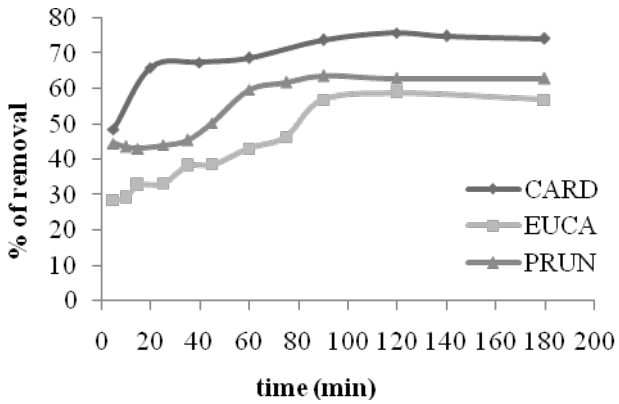

Fig. 7. Percentage of RN removal vs. time for the three biosorbents (C_0 = 100 mg L^{-1}).

The intraparticle diffusion model can be expressed as follows:

$$q_t = K_{int}\, t^{1/2} + C \quad (5)$$

where K_{int} (mg g^{-1} min$^{-1/2}$) is the intraparticle diffusion rate constant, and C (mg g^{-1}) is the intercept. The value of C gives an idea about the thickness of the boundary layer: the larger the intercept, the greater the boundary layer effect. The plots q_t vs. $t^{1/2}$ are shown in Fig. 9.

The computed constants (experimental and calculated values) that have a direct correlation with the adsorption speed are reported in Table 2.

The sum of squares error (SSE, %) is one method that has been used in literature to test the validity of each model. The SSE is given as:

$$\mathrm{SSE}(\%) = \sqrt{\sum \left[(qe)\exp - (qe)\mathrm{cal}\right]^2 / N} \quad (6)$$

where N is the number of data points.

The low values of the regression coefficient (R^2) of the first-order kinetic model suggest that the adsorption obeys this type of kinetics. The adsorption capacities confirm this hypothesis, since their values graphically obtained do not

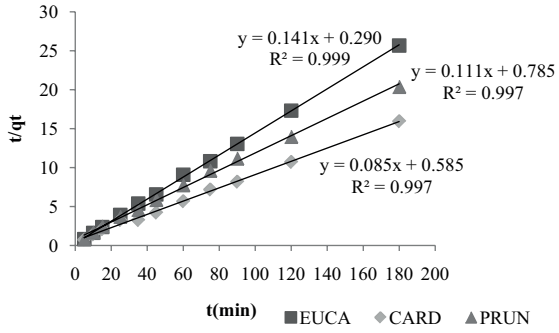

Fig. 8. Pseudo-second-order kinetic models for the biosorption of RN by the three biosorbents: *Eucalyptus globulus* (■), *Cynara cardunculus* (♦), and *Prunus cerasefera* (▲) – initial concentration of 100 mg L^{-1}.

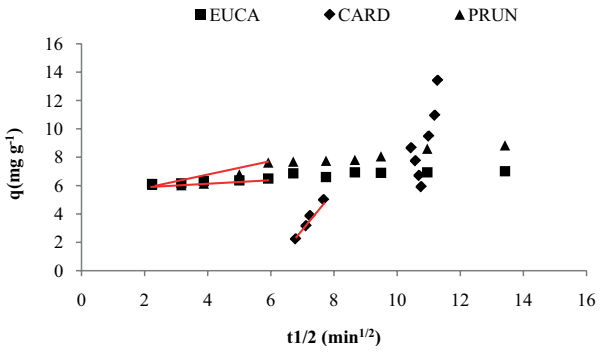

Fig. 9. Intraparticle diffusion of RN by the three biosorbents: *Eucalyptus globulus* (■), *Cynara cardunculus* (♦), and *Prunus cerasefera* (▲).

Table 2
Results of the adsorption kinetics of red nylosane

		Eucalyptus globulus	*Cynara cardunculus*	*Prunus cerasifera*
C_0 (mg L^{-1})		100	100	100
q_e (exp) (mg g^{-1})		7.011	11.284	8.838
Pseudo-first order	q_e (calc) (mg g^{-1})	0.9582	4.8739	3.2362
	k_1 (min^{-1})	0.0237	0.0325	0.0192
	R^2	0.8094	0.8455	0.9201
	SSE (%)	4.279	4.862	4.082
Pseudo-second order	q_e (calc) (mg g^{-1})	7.0621	11.7508	9.0090
	k_2 (g/mg min)	0.0699	0.0134	0.0162
	H (mg/g min)	3.4387	1.707	1.2724
	R^2	0.9997	0.9971	0.9972
	SSE (%)	0.036	0.330	0.121
Intraparticle diffusion	K_{int} (mg g^{-1} $min^{-1/2}$)	0.0985	0.3122	0.2678
	C	5.8873	6.0878	5.2947
	R^2	0.9018	0.9867	0.7463

correspond to those experimentally found. Indeed, in terms of the biosorbent from CARD, the adsorption capacity is calculated graphically from 11.28 mg g^{-1}; by against experimentally, it is equal to 4.87 mg g^{-1}.

From Fig. 8, the pseudo second order is the appropriate model for the adsorption of RN, since the values of correlation coefficient R^2 are close to unity. This is confirmed by the fact that the values of the maximum experimental adsorption and graphics are very close to when the pseudo-second order (Table 2). The same results are found by other researchers in different dyes students like: adsorption on activated carbon derived from sawdust [31] and the elimination of Congo red by coal coconut husk [32].

The values of SSE (%) for the pseudo-first and pseudo-second kinetic models are given in Table 2. It can be seen that the SSE (%) values are lower for the second-order kinetic model with respect to those for the pseudo-first-order model, which confirms the better applicability of the pseudo-second-order model.

The diffusion rate of intraparticle has two stages as shown in Fig. 9; the first step can be attributed to the rapid spread of the adsorbent with the solution on the outer surface of the adsorbent (plateau). This step is followed by a plateau-like step (phase 2) that can be attributed to the final stage of equilibrium.

The parameters K_{int} and C are determined from the first-stage linear. The parameter C is proportional to the thickness of the boundary layer. Note for most systems the value of C increases, this increase is the increase of the thickness of the boundary layer [29]. However, the best model to fit the adsorption kinetics of the three biosorbents is the pseudo-second-order model.

3.5. Adsorption isotherm of RN

Time, dose, and pH, these parameters were set identified to establish the adsorption isotherm of RN on different systems; 25 mL solutions of initial concentrations ranging from 50 to 1,000 mg L^{-1} were mixed with an optimal dose of each biosorbent.

The adsorption isotherm is a plot of the amount adsorbed per unit mass of biosorbents that are studied in function of the concentration RN in equilibrium at room temperature. There are various equations to describe the adsorption isotherms. The most equations used are the Langmuir and Freundlich model, which are, respectively, represented as linear Eqs. (7) and (8):

$$\frac{C_{eq}}{q} = \frac{1}{b}C_{eq} + \frac{1}{K_L b} \tag{7}$$

$$\log q = \frac{1}{n}\log C_{eq} + \log K_F \tag{8}$$

The results of adsorption of RN by the different systems are plotted in Fig. 10.

As shown in the figures, these isotherms obey the Langmuir Fig. 10(b) and Freundlich model Fig. 10(c) for all systems with satisfactory correlation coefficients. The largest adsorption capacity was obtained for the biosorbent, which is derived from CARD and EUCA with an adsorption capacity of 83.33 mg g^{-1} followed by PRUN with an adsorption capacity of 76.92 mg g^{-1}, indicating our biosorbents prepared in the laboratory, they are good precursors and well performed in comparison with the commercial activated carbon (Aldrich; 400 mg g^{-1}). Table 4 summarizes the results of biosorption for both models studied as well as other work done by researchers [33].

K_L constant calculated from the Langmuir model indicates the affinity between the adsorbent and the adsorbate; thus, a large value of K_L implies the presence of a strong bond between the adsorbent and the adsorbate. As can be seen in Table 3, the value of K_L for CARD in the simple solution is 0.008 L mg^{-1} is higher than that of EUCA (0.0058 L mg^{-1}) and PRUN. It can be explained by the phenomenon of number of adsorption sites that biosorbent has a different one other.

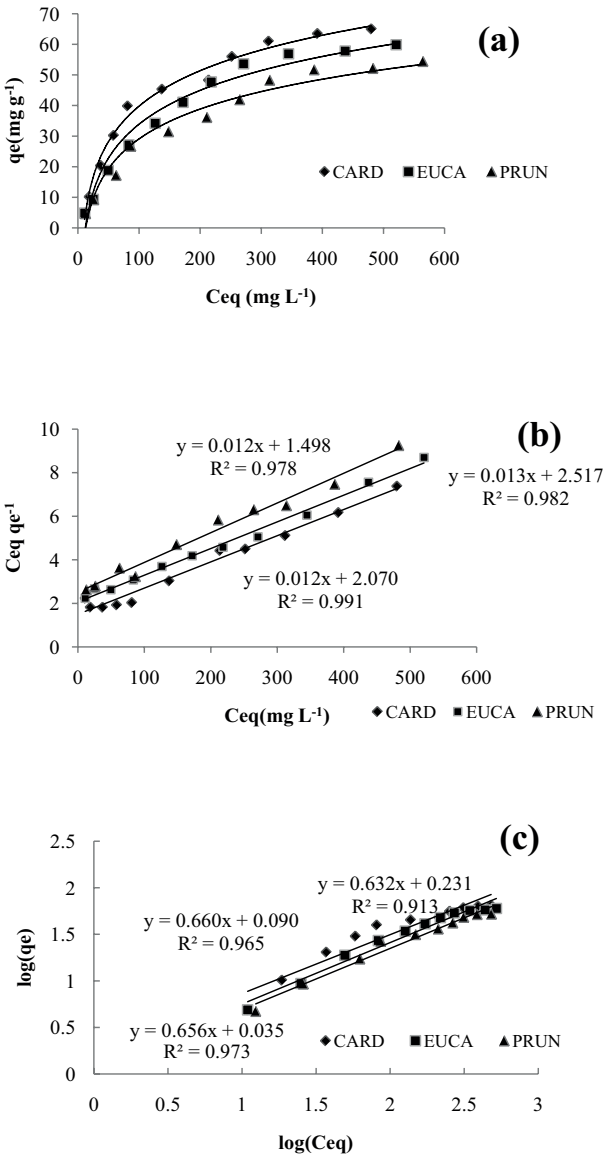

Fig. 10. Isothermal adsorption of red nylosane with three biosorbents (a), Isotherm of Langmuir (b), Isotherm of Freundlich (c): *Eucalyptus globulus* (■), *Cynara cardunculus* (♦), and *Prunus cerasefera* (▲).

Freundlich constants K_F and n are also calculated, from the model of Eq. (8) of Freundlich. The value of n calculated for the adsorption in the solution increases; as an example for RN, the value of n is greater than 1 indicates that the RN is favorably adsorbed by the three biosorbents.

The value of K_F is significant for each biosorbents. It gives an explanation that these systems also obey the Freundlich model, indicating some heterogeneity of the adsorbent surface with correlation coefficients of 0.96 and 0.973 for both biosorbents PRUN and EUCA, respectively, and 0.913 for the biosorbent CARD, with a constant n in the range from 28.57 to 11.11 and 4.33 successively.

3.6. Study of the influence of temperature on the adsorption process of the RN

The thermodynamic parameters are important for understanding the effect of temperature on adsorption.

In adsorption, the physical–chemical reactions give the relationship between the equilibrium constant and the temperature under the assumption in which $\Delta H°$ is constant in the range studied and temperature can be expressed by the equation of van 't Hoff:

The thermodynamic parameters of adsorption, like $\Delta G°$ and $\Delta S°$, can also be obtained from the following equations:

$$\Delta G = -RT \ln Kd \tag{9}$$

$$\ln Kd = \frac{\Delta S}{R} - \frac{\Delta H}{RT} \tag{10}$$

where Kd is the equilibrium constant; T is the absolute temperature (K); $\Delta H°$ is the enthalpy (kJ/mol); and R is the universal gas constant (8.314 J/K mol).

Kd is the distribution coefficient calculated from Eq. (11):

$$Kd = \frac{C_{eqs}}{C_{EQ}} \tag{11}$$

where C_{eqs} is the amount of dye (mg) adsorbed on the adsorbent per liter of the solution at equilibrium, and C_{EQ} is the equilibrium concentration (mg L^{-1}) of the dye in the solution.

Table 3
Langmuir constants and Freundlich adsorption red nylosane

Component	Biosorbents	Langmuir constants			Freundlich constants			Reference
		q_{max} (mg g^{-1})	K_L (L mg^{-1})	R^2	K_F	n	R^2	
Red nylosane	CARD	83.33	0.008	0.978	1.88	4.33	0.913	Our work
	PRUN	76.92	0.0052	0.982	1.92	28.57	0.973	Our work
	EUCA	83.33	0.0058	0.991	1.93	11.11	0.965	Our work
	Carbon (Aldrich)	400	0.02	0.97	18.66	1.92	0.8	Our work
	Carbons prepared from coffee grounds by H_3PO_4 activation	367	0.077	–	–	–	–	[34]

The value of $\Delta H°$ was calculated from the slope of the linear regression of ln$K$ as a function of 1/T (Fig. 11). Estimated thermodynamic parameters such as $\Delta H°$, $\Delta S°$ and $\Delta G°$ at each temperature are summarized in Table 4.

The enthalpy change ($\Delta H°$) for the adsorption of RN on the three biosorbents means an endothermic adsorption. Similar results were reported for adsorption on bentonite [34], activated carbon prepared from defatted soybean and activated carbon prepared from Tunçbilek lignite [35,36]. $\Delta G°$ values were reduced when the temperature rose from 25°C to 55°C, suggesting an increase in the adsorption of RN with increasing temperature [27]. The positive value of $\Delta S°$ reflects the affinity of the three biosorbents vis-à-vis the RN [13,36] and also suggests that the degree of freedom increases the solid–solution interface.

These results show that the process of adsorption on different adsorbents is done with spontaneous and favorable reactions ($\Delta G° < 0$), thus confirming the affinity of the biosorbents for the dye. The values of the heat of adsorption obtained from our samples affirm that the interactions with the dye RN are chemical for all systems. Also imply the existence of the flexible connections between the molecules and the surface of RN biosorbent [37].

4. Conclusion

This present work was oriented to the study of the elimination of organic micropollutants "Red Nylosane" of water using three biosorbents in their raw state EUCA, CARD and PRUN.

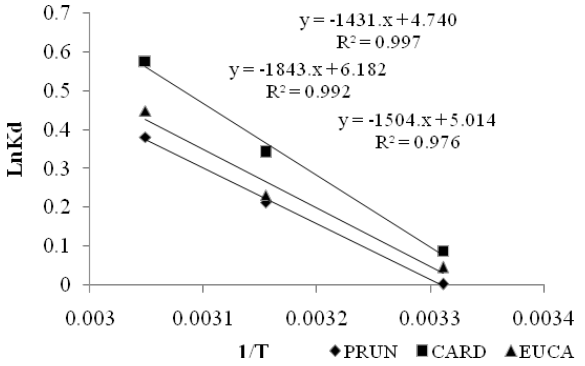

Fig. 11. Effect of temperature on adsorption of RN by the three biosorbents.

Table 4
Results of the effect of temperature on adsorption of red nylosane by the three biosorbents (C_0 = 200 mg L^{-1})

Biosorbent	$\Delta G°$ (kJ/mol)			$\Delta H°$ (kJ/mol)	$\Delta S°$ (kJ/mol K)
	Temperature (K)				
	302	317	328		
CARD	–0.22	–0.90	–1.57	15.3	0.051
EUCA	–0.11	–0.61	–1.22	11.9	0.039
PRUN	–0.01	–0.56	–1.04	12.5	0.025

We used different methods to characterize the surface of biosorbents prepared by FTIR analysis, which confirms the presence of alcoholic functional groups, carboxylic acid and amine groups that chemically interact with RN anions and thus play an important role in the adsorption process. The characterization of materials for microporosity by determining the value of the iodine number. The value determines the maximum of 535 mg g^{-1} for CARD followed by EUCA (446 mg g^{-1}) and PRUN of 370 mg g^{-1}. Determining the surface area available to methylene blue, which revealed to obtain a surface of 746 m^2 g^{-1} for the biosorbent CARD that represents great value followed by EUCA (560 m^2 g^{-1}) and PRUN (320 m^2 g^{-1}), was very large compared with the BET surface area (22, 14, and 13.8 m^2 g^{-1}, respectively). It was found that each gram of both biosorbents EUCA and CARD adsorbed 83.33 mg g^{-1}, against 76.92 mg g^{-1} for PRUN leaves at an optimum pH of 2. The adsorption isotherms obey the Langmuir equation with a very rapid initial phase, and the balance was checked at 120 min.

The pseudo-second-order kinetic model is the most adapted to describe the adsorption process.

The process of adsorption of RN on the three biosorbents is spontaneous and endothermic. This study showed that the biosorbents are an excellent example of economic use of plant waste to environmental protection without any drawbacks and can be used for the removal of organic micropollutants from textiles releases.

References

[1] J.G. Dean, F.L. Basqui, K.H. Lanouette, Adsorption of iron and manganese ions using low-cost materials as adsorbents, Environ. Sci. Technol., 6 (1972) 509.
[2] D.P. Tiwari, K. Romod, A.K. Mishra, R.P. Singh, Srivastov, Removal of toxic metals from electroplating industries, Indian J. Environ. Health, 31 (1989) 120–124.
[3] M. Termoul, B. Bestani, N. Benderdouche, M. Belhakem, E. Naffrechoux, Removal of phenol and 4-chlorophenol from aqueous solutions by olive stone-based activated carbon, Adsorpt. Sci. Technol., 24 (2006) 375–387.
[4] B. Bestani, N. Benderdouche, B. Benstaali, A. Addou, Methylene blue and iodine adsorption onto an activated desert plant, Bioresour. Technol., 99 (2008) 8441–8444.
[5] N. Benderdouche, B. Bestani, B. Benstaali, D. Derriche, Enhancement of the adsorptive properties of a desert Salsola Vermiculata species, Adsorpt. Sci. Technol., 21 (2003) 739–750.
[6] A. Ouldmoumna, L. Reinert, N. Benderdouche, B. Bestani, L. Duclaux, Characterization and application of three novel biosorbents "*Eucalyptus globulus*, *Cynara cardunculus*, and *Prunus cerasefera*" to dye removal, Desal. Wat. Treat., 51 (2013) 3527–3538.
[7] M.C. Ncibi, B. Mahjoub, M. Seffen, Kinetic and equilibrium studies of methylene blue biosorption by *Posidonia oceanica* (L.) fibres, J. Hazard. Mater., 139 (2007) 280–285.
[8] F.A. Batzias, D.K. Sidiras, Dye adsorption by calcium chloride treated beech sawdust in batch and fixed-bed systems, J. Hazard. Mater., 114 (2004) 167–174.
[9] V. Dulman, S. Cucu-Man, V.I. Popa, R. Mureşan, Adsorption properties of beech wood sawdust related to some textile dyes, J. Anal. Şt. Univ. "Al. I. Cuza" Iaşi VIII, 8 (2000) 245–252.
[10] V.K. Kumar, S. Sivanesan, Isotherms for Malachite Green onto rubber wood (*Hevea brasiliensis*) sawdust: comparison of linear and non-linear methods, Dyes Pigm., 72 (2007) 124–129.
[11] F. Ferrero, Dye removal by low cost adsorbents: hazelnut shells in comparison with wood sawdust, J. Hazard. Mater., 142 (2007) 144–152.

[12] O. Hamdaoui, Batch study of liquid-phase adsorption of methylene blue using cedar sawdust and crushed brick, J. Hazard. Mater., 135 (2006) 264–273.
[13] N. Yeddou, A. Bensmaili, Kinetic models for the sorption of dye from aqueous solution by clay-wood sawdust mixture, Desalination, 185 (2005) 499–508.
[14] V.K. Garg, M. Amita, R. Kumar, R. Gupta, Basic dye (methylene blue) removal from simulated wastewater by adsorption using Indian Rosewood sawdust: a timber industry waste, Dyes Pigm., 63 (2004) 243–250.
[15] S. Chakraborty, S. De, J.K. Basu, S. DasGupta, Treatment of a textile effluent: application of a combination method involving adsorption and nanofiltration, Desalination, 174 (2005) 73–85.
[16] I. Safarik, M. Safarikova, F. Weyda, E. Mosiniewicz-Szablewska, A. Slawska-Waniewska, Ferrofluid-modified plant-based materials as adsorbents for batch separation of selected biologically active compounds and xenobiotics, J. Magn. Magn. Mater., 293 (2005) 371–376.
[17] V. Dulman, S.M. Cucu-Man, Sorption of some textile dyes by beech wood sawdust, J. Hazard. Mater., 162 (2009) 1457–1464.
[18] Y. Azila Yahaya, M. Mat Don, Biosorption of copper (II) onto immobilized cells of *Pycnoporus sanguineus* from aqueous solution: equilibrium and kinetic studies, J. Hazard. Mater., 161 (2009) 189–195.
[19] M.A. Ashraf, M. Hussain, K. Mahmood, A. Wajid, M. Yusof, Y. Alias, I. Yusoff, Removal of acid yellow-17 dye from aqueous solution using eco-friendly biosorbent, Desal. Wat. Treat., 51 (2013) 4530–4545.
[20] M.C. Ncibi, A.M. Ben Hamissa, A. Fathallah, M.H. Kortas, T. Baklouti, B. Mahjoub, M. Seffen, Biosorptive uptake of methylene blue using Mediterranean green alga *Enteromorpha* spp., J. Hazard. Mater., 170 (2009) 1050–1055.
[21] A.E. Ofomaja, Y.-S. Ho, Effect of temperatures and pH on methyl violet biosorption by Mansonia wood sawdust, Bioresour. Technol., 99 (2008) 5411–5417.
[22] C.-H. Weng, Y.-T. Lin, T.-W. Tzeng, Removal of methylene blue from aqueous solution by adsorption onto pineapple leaf powder, J. Hazard. Mater., 170 (2009) 417–424.
[23] R. Perrin, J. Pscharff, Industrial Chemistry, 2nd ed., Dunod, Paris, 1999, pp. 661–679.
[24] ASTM, Standard Test Method for Determination of Iodine Number of Activated Carbon, Vol. 4, Section 15, ASTM Annual Book, 1999, D4607-94.
[25] J. Jagiello, J.P. Olivier, A simple two-dimensional NLDFT model of gas adsorption in finite carbon pores. Application to pore structure analysis, J. Phys. Chem. C, 113 (2009) 19382–19385.
[26] J. Zawadzki, Infrared Spectroscopy in Surface Chemistry of Ethylene, P.A. Thrower, Ed., Chemistry and Physics of Carbon, Vol. 21, Marcel Dekker, New York, 1989, pp. 147–386.
[27] J.X. Lin, S.L. Zhan, M.H. Fang, X.Q. Qian, H. Yang, Adsorption of basic dye from aqueous solution onto fly ash, J. Environ. Manage., 87 (2008) 193–200.
[28] S.D. Khattri, M.K. Singh, Removal of malachite green from dye wastewater using neem sawdust by adsorption, J. Hazard. Mater., 167 (2009) 1089–1094.
[29] B.H. Hameed, M.I. El-Khaiary, Malachite green adsorption by rattan sawdust: isotherm, kinetic and mechanism modeling, J. Hazard. Mater., 159 (2008) 574–579.
[30] B.H. Hameed, Spent tea leaves: a new non-conventional and low-cost adsorbent for removal of basic dye from aqueous solutions, J. Hazard. Mater., 161 (2009) 753–759.
[31] P.K. Malik, Dye removal from wastewater using activated carbon developed from sawdust: adsorption equilibrium and kinetics, J. Hazard. Mater., 113 (2004) 81–88.
[32] C. Namasivayam, D. Kavitha, Removal of Congo Red from water by adsorption onto activated carbon prepared from coir pith, an agricultural solid waste, Dyes Pigm., 54 (2002) 47–58.
[33] A. Reffas, V. Bernadet, B. David, L. Reinert, M.B. Lehocine, M. Dubois, N. Batisse, L. Duclaux, Carbons prepared from coffee grounds by H_3PO_4 activation: characterisation and adsorption of methylene blue and Nylosane Red N-2RBL, J. Hazard. Mater., 175 (2010) 779–788.
[34] M.-H. Baek, C. Olakitan Ijagbemi, S.-J. O, D.-S. Kim, Removal of Malachite Green from aqueous solution using degreased coffee bean, J. Hazard. Mater., 176 (2010) 820–828.
[35] S.S. Tahir, N. Rauf, Removal of a cationic dye from aqueous solutions by adsorption onto bentonite clay, Chemosphere, 63 (2006) 1842–1848.
[36] Y. Onal, C. Akmil-Basar, D. Eren, C .Sarici-Ozdemir, T. Depci, Adsorption kinetics of malachite green onto activated carbon prepared from Tuncbilek lignite, J. Hazard. Mater., 128 (2006) 150–157.
[37] D. Sigh, Studies of the adsorption thermodynamics of oxamyl on fly ash, Adsorpt. Sci. Technol., 18 (2000) 741–748.